e-Prime - Advances in Electrical Engineering, Electronics and Energy 6 (2023) 100295

Contents lists available at ScienceDirect

e-Prime - Advances in Electrical Engineering, Electronics and Energy

journal homepage: www.elsevier.com/locate/prime

Fractional order controller design via gazelle optimizer for efficient speed regulation of micromotors

Davut Izci [a,b,*], Serdar Ekinci [a]

[a] Department of Computer Engineering, Batman University, Batman, 72100, Turkey
[b] MEU Research Unit, Middle East University, Amman, Jordan

ARTICLE INFO

Keywords:
Micro DC motor
Speed regulation
FOPID controller
Gazelle optimization algorithm
Metaheuristics

ABSTRACT

In this paper, the design of an efficient fractional-order proportional-integral-derivative (FOPID) controller, tailored specifically for the regulation of micro direct current (DC) motors, is explored. A fresh approach is introduced using the gazelle optimization algorithm (GOA), a cutting-edge method set to manage the speed control of these small but vital motors. With the adoption of GOA, fine-tuning the parameters of the FOPID controller is aimed. This is achieved by employing a time-based performance metrics-based cost function as the guiding compass. The GOA is implemented to discover the optimal controller settings for the attainment of peak performance. Through thorough simulations and careful statistical analysis, the worth of GOA-based FOPID controller is demonstrated. Not only are top-notch cost function values achieved, but excellence across various time domain-based performance metrics is also excelled in. The results suggest that the GOA proves to be efficient in fine-tuning of FOPID controller parameters. A comprehensive analysis in the time domain further solidifies the superiority of GOA-based FOPID-controlled micro-DC motor system. Outperformance is observed when compared to alternative algorithms employing different controllers, such as an advanced hybrid stochastic fractal search-based FOPID controller, a grey wolf optimizer-based FOPID controller, a slime mold algorithm-based PID controller, an enhanced arithmetic Harris hawks optimization-based PID controller, and a hybrid atom search optimization and simulated annealing-based PID controller. In essence, the results highlight the potential of the GOA as a powerful tool poised to reshape the optimization of FOPID controllers for micro-DC motor speed regulation.

1. Introduction

1.1. Background

Micro-DC motors are diminutive yet potent devices that play a pivotal role in a wide array of industries and applications [1]. These compact electrical motors are deployed in diverse fields such as robotics, automotive technology, medical devices, and consumer electronics. Their significance lies in their ability to precisely control rotational speed, which is crucial for ensuring the efficiency, accuracy, and functionality of various mechanisms. Whether it's maintaining the stability of a miniature drone, providing precise motion control in medical instruments, or achieving autofocus in cameras, the capacity to regulate the speed of micro-DC motors is paramount [2]. In this context, this article delves into the world of micro-DC motors, their extensive application fields, and underscores the critical importance of speed regulation in harnessing their capabilities for innovation and performance enhancement.

1.2. Literature

Micro-DC motors are highly regarded for their ease of control, exceptional durability, and cost-efficiency. In numerous industries that employ these compact motors, precise speed regulation stands as a fundamental requirement. Given their crucial role as primary actuation components in dynamic systems, achieving accurate speed regulation is imperative. To this end, a variety of control structures have been adopted, including the proportional-integral (PI) controller [3,4], proportional-derivative (PD) controller [5], proportional-integral-derivative (PID) controller [6], fuzzy PID controller [7,8], fractional order PID (FOPID) controller [9], and adaptive controller [10], all geared towards optimizing speed regulation for DC motors.

* Corresponding author.
E-mail addresses: davutizci@gmail.com, davut.izci@batman.edu.tr (D. Izci), serdar.ekinci@batman.edu.tr (S. Ekinci).

https://doi.org/10.1016/j.prime.2023.100295
Received 6 August 2023; Received in revised form 12 September 2023; Accepted 20 September 2023
Available online 22 September 2023
2772-6711/© 2023 The Author(s). Published by Elsevier Ltd. This is an open access article under the CC BY-NC-ND license (http://creativecommons.org/licenses/by-nc-nd/4.0/).

Among these control structures, PID controllers have consistently occupied a prominent position in various reported configurations [11]. They have not only played a pivotal role in regulating DC motor speed but have also found widespread application across diverse industrial domains [12–14]. The enduring popularity of PID controllers can be attributed to their cost-effectiveness and user-friendly applicability, coupled with a simple yet reliable design. However, recent advancements have introduced FOPID controllers, which outperform traditional PID controllers in terms of control performance [15]. Optimized FOPID controllers employ advanced algorithms and optimization techniques to finely tune their parameters, thereby achieving specific control objectives. The adoption of these controllers offers enhanced flexibility and has the potential to significantly enhance control performance, particularly in intricate systems characterized by nonlinear dynamics or time-varying parameters [16–20].

To harness the benefits of FOPID controllers effectively, a suitable tuning method is essential. In this context, metaheuristic algorithms have emerged as potent artificial intelligence optimization techniques [21]. Researchers have explored various artificial intelligence techniques to fine-tune FOPID controllers for DC motor systems. For example, the study in [22] explores the design and optimization of both PID and FOPID controllers for speed regulation in a chopper-fed DC motor drive. Controllers are designed in both time and frequency domains, aiming to minimize rise time, settling time, and maintain iso-damping characteristics. An enhanced artificial bee colony (ABC) algorithm with opposition search is employed for optimization, allowing users to choose controllers based on specific requirements. Comparative analysis highlights the advantages of fractional order controllers over conventional PID schemes, and the study demonstrates the effectiveness of the opposition-based ABC method through computer simulations and extensive analysis. In [23], the atom search optimization (ASO) algorithm and its novel chaotic version, chaotic ASO (ChASO), are introduced for optimizing the parameters of a FOPID controller in the context of DC motor speed control. The comparative analysis includes the application of ChASO to benchmark optimization problems and a comprehensive comparison of ChASO-FOPID, ASO-FOPID, and ASO-PID controllers with other established controllers, demonstrating superior performance in terms of various objective functions, transient response, frequency response, and robustness in simulations. The work in [24] presents the design of a FOPID for DC motor speed regulation, emphasizing the advantages of FOPID over conventional PID controllers, particularly in handling higher-order systems. FOPID is highlighted for its Iso-damping property, enhancing the system's robustness against gain variations. The study employs the particle swarm optimization (PSO) to fine-tune FOPID controller parameters, with a focus on minimizing peak overshoot, rise time, and settling time. Simulation results validate the effectiveness of the FOPID controller, showcasing its robustness and control performance when compared to the conventional PID controller. Finally, in [9], FOPID controller is also applied to regulate the speed of a DC motor. The controller's parameters are optimized using a novel metaheuristic algorithm called opposition-based learning hybrid manta ray foraging optimization with simulated annealing (OBL-MRFO-SA). Comprehensive analyses, including time and frequency domain simulations, robustness testing, and load disturbance rejection, demonstrate the superiority of the OBL-MRFO-SA algorithm compared to other state-of-the-art optimization techniques. Additionally, the algorithm's effectiveness is validated using a physical setup, further affirming its outstanding performance in DC motor speed control.

1.3. Motivation and contributions

In the preceding section, we have listed notable improvements achieved through various methods. However, as the "no free lunch" theorem [25] wisely reminds us, there is no universal cure applicable to all scenarios. This leaves room for continuous enhancements and innovations. In the pursuit of this objective, our study endeavors to introduce a fresh and intelligent optimization approach for crafting an efficient FOPID controller tailored to the demands of a micro-DC motor system.

In this endeavor, we have adopted the gazelle optimization algorithm (GOA) [26] as our innovative tuning instrument. The GOA stands out as a novel metaheuristic algorithm, drawing inspiration from the remarkable survival instincts of gazelles in their natural habitat. Gazelles, renowned for their ability to outmaneuver and outpace predators, inspire the GOA's modeling. This algorithm has demonstrated success across a spectrum of optimization problems [26–28].

The motivation of this study revolves around applying the GOA to fine-tune the FOPID controller for the regulation of a micro-DC motor's speed. Here, we present an extensive exploration into the integration of the FOPID controller with an externally excited micro-DC motor, harnessing the full potential of the GOA for optimal performance. To achieve a feasible and efficient solution for regulating the micro-DC motor's speed, we have framed the problem as a constraint minimization task. The GOA is entrusted with the mission of minimizing the *ZLG* cost function [29], all while adhering to essential time-domain design criteria, including rise time, settling time, peak time, and overshoot.

The GOA-based FOPID controller undergoes rigorous examination through comparative simulations, with meticulous statistical analysis of its performance. These simulations consistently underscore the GOA's ability to achieve superior cost function values and excel in time-domain-based performance metrics, attesting to its efficiency and effectiveness in optimizing FOPID controller parameters. In a comprehensive time-domain-based analysis, the supremacy of GOA-based FOPID-controlled micro-DC motor system is unmistakable. It surpasses the performance of alternative algorithms involving different controllers, including an enhanced hybrid stochastic fractal search based FOPID controller [30], grey wolf optimizer based FOPID controller [31], slime mould algorithm based PID controller [32], enhanced arithmetic Harris hawks optimization based PID controller [33] and hybrid atom search optimization and simulated annealing based PID controller [34]. The results presented in this study underscore the vast potential of the GOA as a potent tool for optimizing the FOPID controller in the realm of micro-DC motor speed regulation.

2. Gazelle optimizer

The gazelle optimization algorithm (GOA) draws inspiration from the remarkable survival strategies of gazelles and applies their adaptive traits to real-world optimization problems [26]. GOA employs gazelles as search agents, represented by an initially randomized $n \times d$ matrix, as shown in Eq. (1) where X denotes the candidate population. The optimizer considers constraints through upper bound (UB) and lower bound (LB) values to define the acceptable range for the population vector.

$$X = \begin{bmatrix} x_{1,1} & x_{1,2} & \cdots & x_{1,d-1} & x_{1,d} \\ x_{2,1} & x_{2,2} & \cdots & x_{2,d-1} & x_{2,d} \\ \vdots & \vdots & x_{i,j} & \vdots & \vdots \\ x_{n,1} & x_{n,2} & \cdots & x_{n,d-1} & x_{n,d} \end{bmatrix} \tag{1}$$

Each position vector $x_{i,j}$ is stochastically generated using Eq. (2) with random number '*rand*', and the problem's upper and lower bounds (UB_j and LB_j).

$$x_{i,j} = rand \times \left(UB_j - LB_j\right) + LB_j \tag{2}$$

To identify the most promising solution, akin to the fittest gazelles in nature excelling in threat detection and evasion, the algorithm designates the best-performing gazelle as the superior solution. This is represented as an Elite $n \times d$ matrix (Eq. (3)) and guides other gazelles during the search process.

$$Elite = \begin{bmatrix} x'_{1,1} & x'_{1,2} & \cdots & x'_{1,d-1} & x'_{1,d} \\ x'_{2,1} & x'_{2,2} & \cdots & x'_{2,d-1} & x'_{2,d} \\ \vdots & \vdots & x'_{i,j} & \vdots & \vdots \\ x'_{n,1} & x'_{n,2} & \cdots & x'_{n,d-1} & x'_{n,d} \end{bmatrix} \quad (3)$$

In the latter definition $x'_{i,j}$ signifies the leading gazelle's position vector. The Elite matrix updates dynamically as better gazelles emerge. For efficient exploration, controlled Brownian motion is employed, described by a Gaussian probability distribution function with variance (σ^2) of 1 and mean (μ) of 0 (Eq. (4)).

$$f_B(x, \mu, \sigma) = \frac{1}{\sqrt{2\pi\sigma^2}} e^{\left(\frac{-(x-\mu)^2}{2\sigma^2}\right)} = \frac{1}{\sqrt{2\pi}} e^{\left(\frac{-x^2}{2}\right)} \quad (4)$$

During grazing, gazelles' movements are modeled by the mathematical expression in Eq. (5), combining random steps to simulate Brownian motion [28].

$$g_{i+1} = g_i + s \cdot R * \cdot R_B * \cdot (Elite_i - R_B * \cdot g_i) \quad (5)$$

In the given context, g_{i+1} denotes the solution achieved in the subsequent iteration, while g_i represents the solution obtained in the current iteration. The parameter "s" characterizes the grazing speed of the gazelles. The vector R_B comprises random numbers designed to simulate Brownian motion, whereas R consists of uniform random numbers ranging from 0 to 1. When a predator is detected, the exploration shifts to Lévy flight, involving both short steps and occasional long jumps. The Lévy distribution is described by Eq. (6), where x_j is the flight distance and α is the power-law exponent which is restricted within the range (1, 2) [28].

$$L(x_j) \approx |x_j|^{1-\alpha} \quad (6)$$

The Lévy stable process is defined as follows [26]:

$$f_L(x; \alpha, \gamma) = \frac{1}{\pi} \int_0^\infty exp(-\gamma q^\alpha) cos(qx) \delta q \quad (7)$$

where the motion is governed by the distribution index (α), and γ represents the scale unit. This optimizer generates stable Lévy motion (Eq. (8)) using α values ranging from 0.3 to 1.99 [28].

$$Levy(\alpha) = 0.05 \times \frac{x}{|y|^{\frac{1}{\alpha}}} \quad (8)$$

The variables α, x, and y are defined as follows: x follows a normal distribution with variance σ_x^2 and mean 0, y follows a normal distribution with variance σ_y^2 and mean 0, and α is set to 1.5. The values of σ_x is calculated as given in (9) and $\sigma_y = 1$ [28].

$$\sigma_x = \left(\frac{\Gamma(1+\alpha)\sin(\pi\alpha/2)}{\Gamma((1+\alpha)/2)\alpha 2^{((\alpha-1)/2)}} \right)^{1/\alpha} \quad (9)$$

The gazelle employs Lévy flight for its escape, while the predator initially adopts Brownian motion before transitioning to Lévy flight. The mathematical description of the gazelle's behavior in spotting the predator is given in Eq. (10) [26].

$$\overrightarrow{g_{i+1}} = \overrightarrow{g_i} + S \cdot \mu \cdot \overrightarrow{R} * \cdot \overrightarrow{R_L} * \cdot \left(\overrightarrow{Elite_i} - \overrightarrow{R_L} * \cdot \overrightarrow{g_i} \right) \quad (10)$$

Here, S represents the top speed that the gazelle can achieve, $\overrightarrow{R_L}$ is a Lévy distribution-based vector of random numbers. The mathematical model in (11) describes the behavior of the predator as it chases the gazelle [26].

$$\overrightarrow{g_{i+1}} = \overrightarrow{g_i} + S \cdot \mu \cdot CF * \cdot \overrightarrow{R_B} * \cdot \left(\overrightarrow{Elite_i} - \overrightarrow{R_L} * \cdot \overrightarrow{g_i} \right) \quad (11)$$

In Eq. (11), CF represents the cumulative effect of the predator, calculated as $CF = (1 - iter/iterMax)^{(2 * iter/iterMax)}$. The predator success rate ($PSRs$) has an impact on the gazelle's ability to escape and prevents local minima trapping. The effect of PSR is modeled in (12) where $\overrightarrow{U}$ is a constructed binary vector generated by a random number r from the interval [0,1], such that $\overrightarrow{U} = 0$ for $r < 0.34$; otherwise $\overrightarrow{U} = 1$. The gazelle matrix contains random indexes of $r1$ and $r2$ [26]. Fig. 1 illustrates a detailed flowchart of GOA.

$$\overrightarrow{g_{i+1}} = \begin{cases} \overrightarrow{g_i} + CF\left[\overrightarrow{LB} + \overrightarrow{R} * \cdot \left(\overrightarrow{UB} - \overrightarrow{LB}\right)\right] * \cdot \overrightarrow{U}; if\ r \le PSRs \\ \overrightarrow{g_i} + [PSRs(1-r) + r](\overrightarrow{g_{r1}} - \overrightarrow{g_{r2}}); else \end{cases} \quad (12)$$

3. Speed regulation of FOPID controlled micromotor

3.1. Mathematical model of externally excited micro-DC motor

This study focuses on a DC motor system consisting of both a micro-DC motor and a mechanical load. The primary objective is to effectively control the speed and torque of the motor through a control system. To create a mathematical model for this system, we have selected a separately excited DC motor [35]. The details of the employed motor, the readers are referred to [36,37]. Fig. 2 depicts the equivalent circuit representing this particular type of DC motor.

To establish a mathematical model, we treat the system as a linear time-invariant one, modeling the mechanical load as a constant torque. Additionally, the motor receives a constant voltage input. Based on these assumptions, we can formulate a set of differential equations that depict the dynamics of the motor's speed and torque. Let ω denote the motor's angular velocity, and τ denote the motor's torque. The dynamics of the system can be described by $J_m(d\omega/dt) = \tau - B_m\omega$ and $L_a(di/dt) = E_a - R_aI_a - K_b\omega$ where J_m is the motor's moment of inertia, B_m is the motor's damping coefficient, L_a is the motor's inductance, R_a is the motor's resistance, K_b is the motor's back electromotive constant, and E_a is the voltage applied to the motor. I_a is the motor's current, which is related to the torque by $\tau = K_m \cdot I_a$, where K_m is the motor's torque constant. These equations can be simplified by assuming that the motor's internal dynamics are much faster than the mechanical load's dynamics. Under this assumption, the motor's angular velocity ω can be assumed to be constant and equal to the commanded speed. With this simplification, the above equations can be reduced to $I_a = (E_a - K_b\omega)/R_a$ for the current. This equation illustrates that the motor's current is directly proportional to the applied voltage and inversely proportional to the motor's resistance. This enables us to control the motor's torque by adjusting the applied voltage. Using this model, we can simulate the system's behavior for various control strategies and load profiles. Additionally, control theory techniques can be applied to design a control system that regulates the motor's speed and torque by modifying the applied voltage. The specific design of such a control system will depend on the unique requirements and constraints of the application. Given the explanation above, we can derive the open-loop transfer function of a DC motor as follows.

$$Plant(s) = \frac{\omega(s)}{E_a(s)} = \frac{K_m}{(L_as + R_a)(J_ms + B_m) + K_mK_b} for\ T_L = 0 \quad (13)$$

3.2. FOPID controller

It is feasible to regulate the speed of a micro-DC motor via a FOPID controller since it is a more flexible controller to control dynamic systems. A FOPID controller is introduced as an improved version of PID [38] that incorporates fractional orders (λ and μ) [39]. FOPID controller's transfer function is defined as follows.

$$FOPID(s) = K_P + \frac{K_I}{s^\lambda} + K_Ds^\mu \quad (14)$$

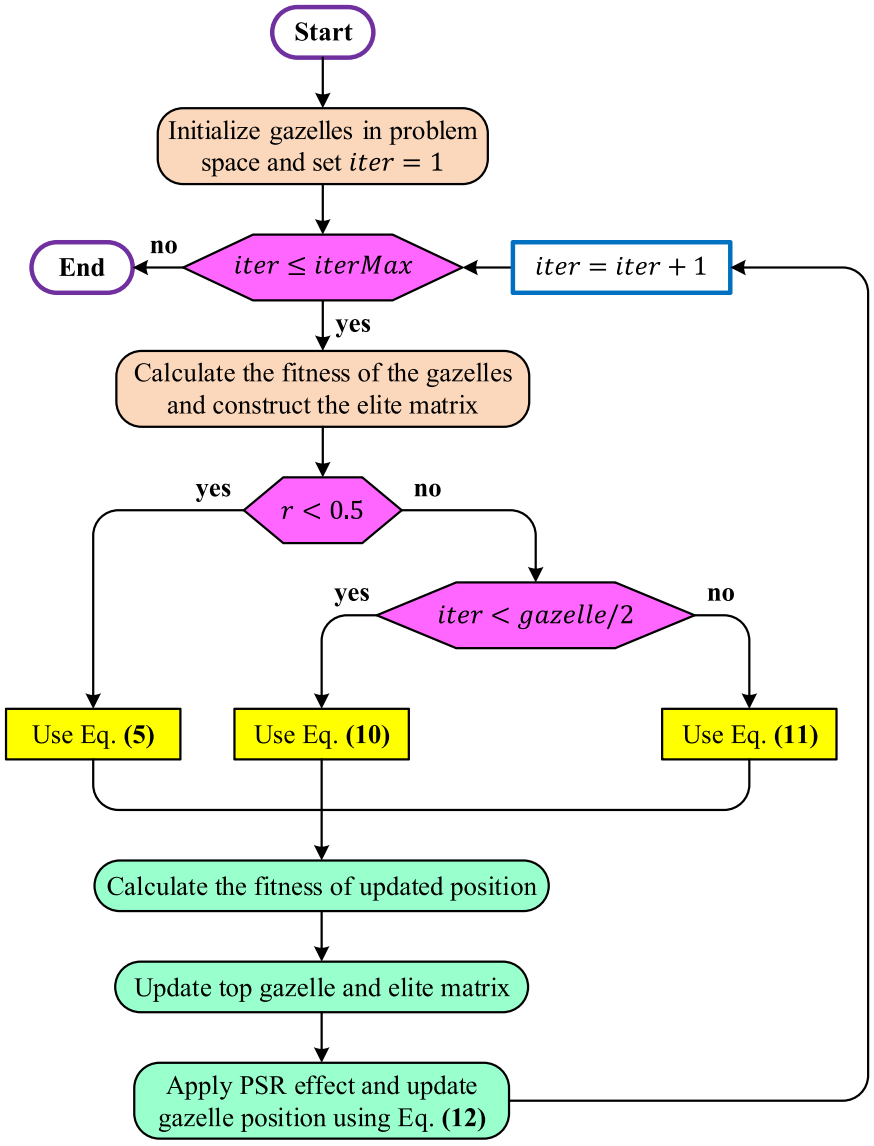


Fig. 1. Flowchart of GOA.

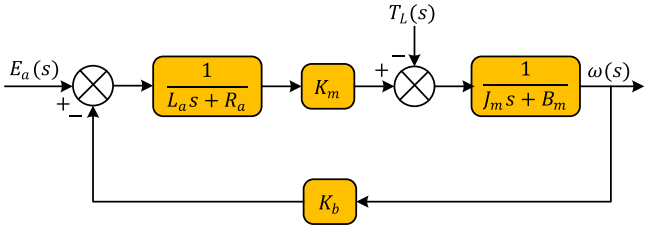


Fig. 2. Equivalent circuit of DC motor.

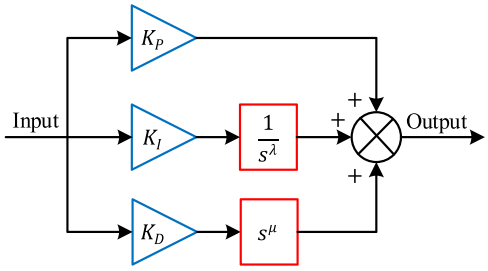


Fig. 3. Block diagram of FOPID controller.

where K_P, K_I, and K_D are proportional, integral, and derivative gains, while λ and μ stand for fractional integral and derivative orders, respectively. Fig. 3 presents the block diagram of a FOPID controller.

3.3. Micro-DC motor speed regulation with FOPID controller

In order to comply with earlier reported studies, we considered the micro-DC motor parameters as 0.40 Ω for R_a, 2.70 H for L_a, 0.0004 $kg{\cdot}m^2$ for J_m, 0.0022 $N{\cdot}m{\cdot}s/rad$ for B_m, 0.015 $N{\cdot}m/A$ for K_m, and 0.05 $V{\cdot}s/rad$ for K_b [30–34]. A FOPID controlled plant can be described with the expression in Eq. (15) [40]. Besides, block diagram of a FOPID controlled DC motor system is illustrated in Fig. 4.

$$T(s) = \frac{\omega(s)}{\omega_{ref}(s)} = \frac{FOPID(s) \times Plant(s)}{1 + FOPID(s) \times Plant(s)} \quad \text{for } T_L = 0 \tag{15}$$

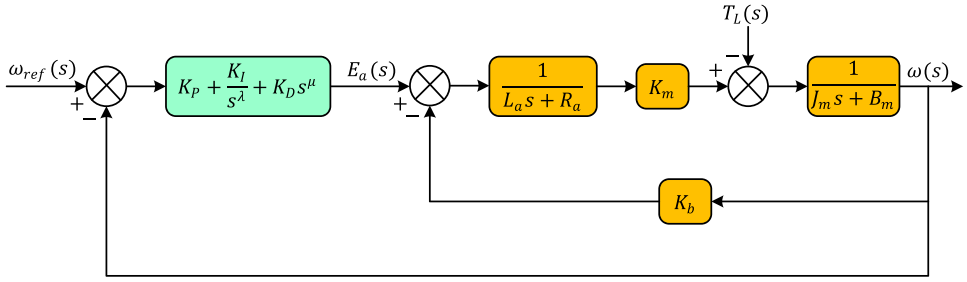


Fig. 4. Block diagram of DC motor system with FOPID controller.

4. A novel design approach for speed regulation of DC motor

4.1. Implementation

We need to describe the speed regulation problem as a minimization problem in order to implement the GOA. In terms of the description of the related system as a minimization problem, the following procedure was adopted in this study so that the parameters of the FOPID controller can be optimized. Firstly, the respective problem was represented as $X = [x_1, x_2, x_3, x_4, x_5] = [K_P, K_I, K_D, \lambda, \mu]$ and secondly the following cost function, known as *ZLG* [29,41], was adopted for appropriate minimization via GOA.

$$ZLG = \left(1 - e^{-\theta}\right) \times \left(SSE + \frac{OS}{100}\right) + e^{-\theta} \times (ST - RT) \tag{16}$$

In here, θ denotes a balancing factor is equal to 1, *SSE* is the steady state error, *OS* is overshoot, *ST* is the settling time and *RT* is the rise time. The bounds adopted for the minimization is presented in Table 2. The proposed GOA based FOPID design strategy for micro-DC motor is illustrated in detail with the bock diagram in Fig. 5. It is worth noting that average elapsed time (per execution) is 33.1792 s for the implementation of the GOA to micro-DC motor speed regulation.

4.2. Statistical superiority

In this section, we assess the statistical performance of the GOA by examining key parameters, constraints, and statistical values. Table 1 provides an overview of the control parameters used for the GOA optimization problem. These parameters include the number of iterations, population size, the number of runs, and other relevant settings. Notably, the population size of 30 individuals and 25 runs were employed to explore the solution space effectively. Additionally, the constraints for the optimization problem are also defined in this table.

Table 2 presents the constraints applied during the optimization process and the parameter values that were fine-tuned using GOA. These constraints help ensure that the optimized parameters fall within predefined limits, contributing to the reliability of the optimization results. Fig. 6 comprises two informative plots. In Fig. 6(a), a stem plot illustrates the performance of the GOA algorithm concerning the cost function. This plot provides a visual representation of the algorithm's progress in minimizing the cost function over iterations. Additionally,

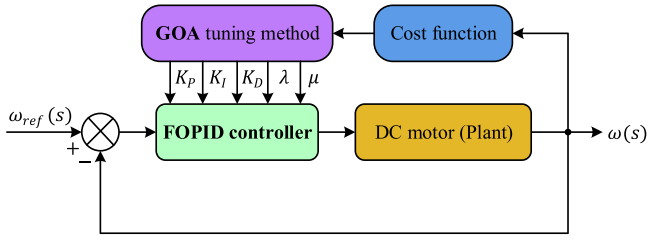


Fig. 5. Block diagram of GOA tuned FOPID controlled system.

Table 1
Control parameters of GOA for optimization problem.

Iteration number	Population size	Number of runs	Other parameters
50	30	25	$s \in [0, 1], \mu \in [-1, 1], S = 0.88$, $PSRs = 0.34$

Table 2
Employed constraints (minimum and maximum) used for the optimization and the tuned parameter values via GOA.

Parameter	Minimum	Maximum	Tuned by GOA
K_P	10	20	19.9016
K_I	0.001	10	7.9640
K_D	0.001	10	9.9979
λ	0.50	1.50	1.0731
μ	0.50	1.50	0.9128

Fig. 6(b) displays a boxplot analysis, offering insights into the distribution of the cost function values obtained by GOA. Finally,

Table 3 summarizes the statistical values associated with the cost function. These values include the best and worst cost function values achieved by the algorithm, the mean cost function value along with its standard deviation, and the median cost function value. Notably, the GOA algorithm has demonstrated its effectiveness in consistently yielding low cost function values, with a best value of 4.2996E−03 and a mean value of 4.3863E−03 ± 6.2366E−05. This statistical analysis underscores the reliability and robustness of GOA in optimizing the given problem, further establishing its superiority in finding high-quality solutions. In summary, the statistical assessment of the GOA algorithm, as presented in these tables and plots, reaffirms its proficiency in optimizing complex problems with precision and consistency, making it a valuable tool for the optimization problem considered in this work.

4.3. Evolutions of controller parameters and cost function

This section explores the dynamic evolution of controller parameters and the associated cost function in the context of optimizing system performance. This analysis is visually represented in Figs. 7 and 8, shedding light on the efficiency and effectiveness of the GOA to optimize FOPID controller parameters for speed control of a micro-DC motor. Fig. 7 portrays the fluctuation of controller parameters over the course of several iterations. This visualization provides valuable insights into how the controller's settings change during the optimization process. Such insights can help engineers and researchers better understand the controller's adaptability and its ability to fine-tune its parameters for optimal system performance. In contrast, Fig. 8 illustrates the variation in the cost function as the optimization algorithm progresses through iterations. The primary objective of this analysis is to demonstrate how the GOA performs in terms of minimizing the cost function. The cost

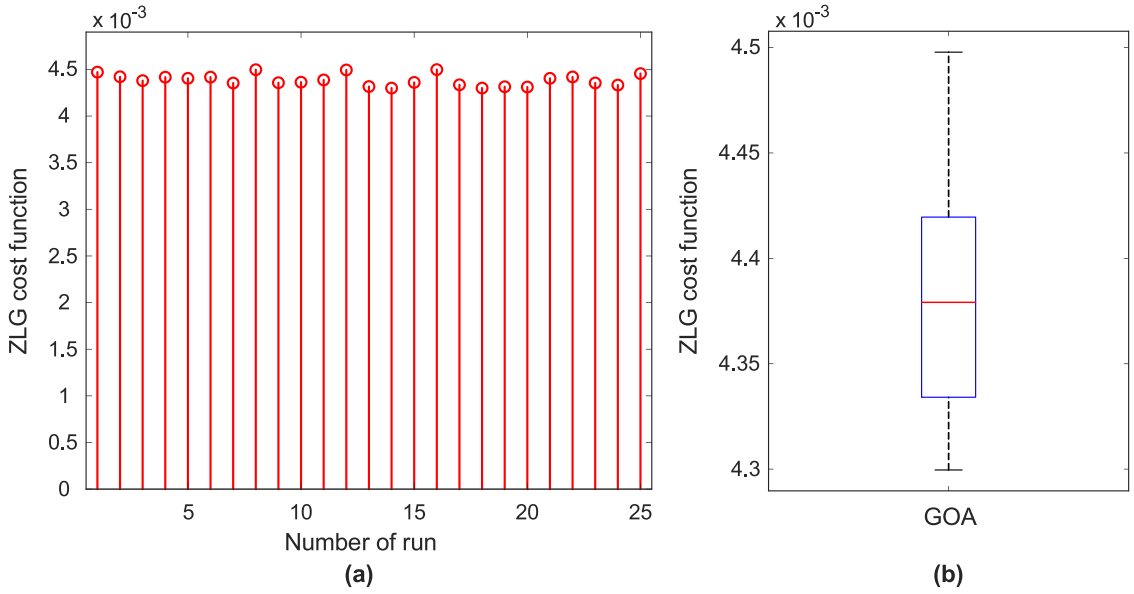


Fig. 6. Stem plot **(a)** and boxplot analysis **(b)** of GOA algorithm for cost function.

Table 3
Statistical values of cost function.

Best	Worst	Mean ± Standard deviation	Median
4.2996E−03	4.4978E−03	4.3863E−03 ± 6.2366E−05	4.3791E−03

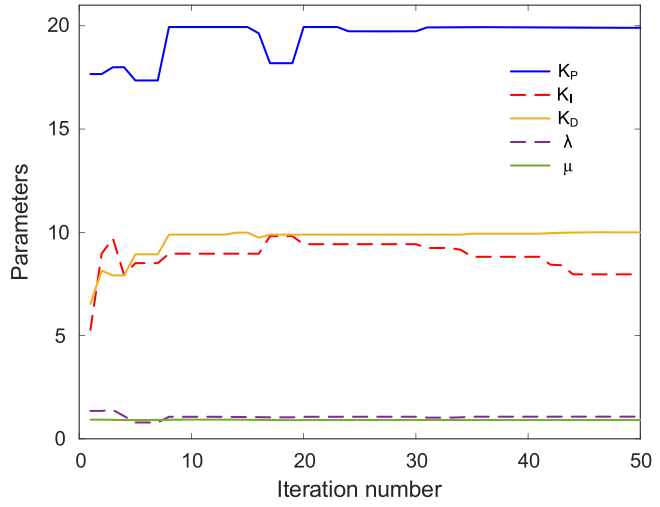


Fig. 7. Variation of FOPID controller parameters with respect to the number of iterations.

function is a critical metric, as it directly reflects the system's efficiency and effectiveness. By examining how this function evolves over time, one can gauge the GOA's capability to reach the lowest possible cost value with increasing iterations. Overall, the information presented in this section and visualized in these figures offers a comprehensive view of the GOA's performance in optimizing controller parameters and ultimately minimizing the cost function. These insights are invaluable for evaluating the algorithm's effectiveness and its potential impact on system control and performance improvement.

4.4. Step response of GOA-FOPID controlled system

In this section, we delve into the step response of the control system

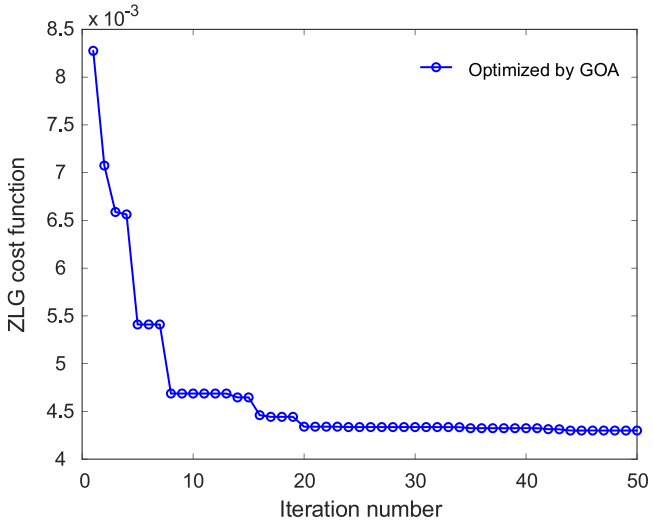


Fig. 8. Variation of cost function with respect to the number of iterations.

when employing the GOA-FOPID tuning approach. This analysis provides invaluable insights into the system's dynamic behavior and its ability to achieve desired performance specifications. Fig. 9 visually illustrates the output speed response of the GOA-FOPID tuned system. This response is indicative of the system's reaction to a step change in the input or setpoint. As depicted in Fig. 9, the output speed response of the GOA-FOPID controlled system is characterized by its remarkable smoothness. The absence of abrupt changes or oscillations in the response curve underscores the GOA-FOPID controller's ability to provide a stable and well-controlled output. Notably, the step response of the GOA-FOPID controlled system shows no overshoot. This means that the output speed settles to its desired value without any initial transient deviation, demonstrating the controller's superior performance in maintaining system stability. The rapid response of the GOA-FOPID controlled system is evident in the quick rise time and settling time. This indicates that the controller efficiently adapts to changes in the setpoint, minimizing the time required to reach and maintain the desired output speed. In summary, the step response analysis of the GOA-FOPID controlled system, as illustrated in Fig. 9, reaffirms the exceptional control capabilities of this tuning approach. Its ability to provide a

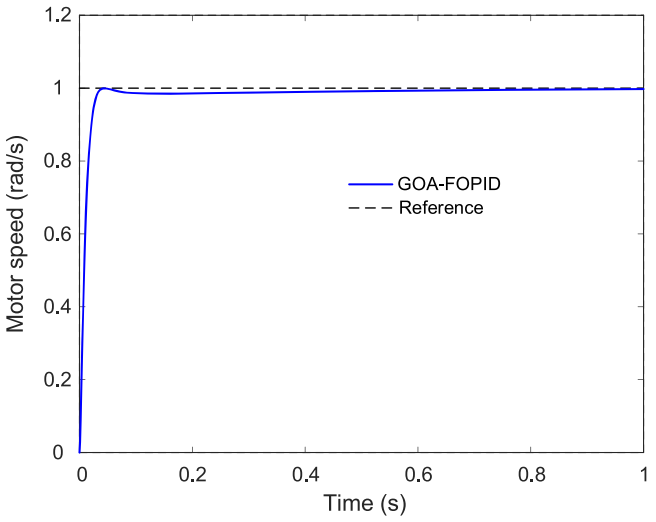


Fig. 9. Output speed response for GOA tuned system.

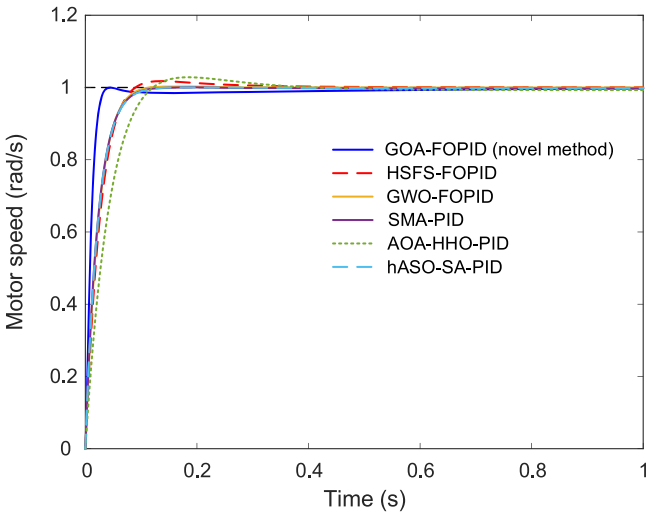


Fig. 10. Comparison of output speed responses for various tuning methods.

smooth response, eliminate overshoot, and achieve rapid settling aligns with the stringent time response specifications often required in practical control applications. These characteristics make the GOA-FOPID controller a promising choice for precise and stable control of dynamic systems.

5. Detailed comparison with reported best works in terms of time response specifications

In this section, we provide a detailed comparison of the GOA-FOPID approach with other state-of-the-art methods, which are considered the best in terms of time response specifications as reported in the literature. The following methods have been adopted for this comparative analysis: an enhanced hybrid stochastic fractal search (HSFS) based FOPID controller [30], grey wolf optimizer (GWO) based FOPID controller [31], slime mould algorithm (SMA) based PID controller [32], enhanced arithmetic Harris hawks optimization (AOA-HHO) based PID controller [33] and hybrid atom search optimization and simulated annealing (hASO-SA) based PID controller [34]. The parameters and their values obtained for these methods are presented in Table 4. It's important to note that for the PID controllers in the table, the fractional orders (λ and μ) are set to 1, as this would convert a FOPID controller into a standard PID controller [42].

In Fig. 10, we illustrate the comparison of output speed responses for various tuning methods, which visually represents the performance differences among these controllers. Table 5 provides a comprehensive performance evaluation, demonstrating the clear superiority of the GOA-FOPID approach over the other reported best methods in terms of time response specifications. Notably, the GOA-FOPID controller exhibits the lowest rise time at 0.0188 seconds and the shortest settling time at 0.0305 seconds, indicating its rapid response to system changes. Moreover, the GOA-FOPID controller achieves zero overshoot, signifying its exceptional ability to maintain stability and eliminate oscillations, a critical factor in many control applications. Additionally, the peak time of 0.044 seconds for the GOA-FOPID controller is the shortest among all methods, emphasizing its ability to reach the peak output response swiftly. These remarkable performance metrics collectively underscore the GOA-FOPID approach as the most effective and efficient method for achieving precise time response specifications in control systems when compared to the alternatives presented in the literature.

Table 4
Controller parameters reported in best approaches (in terms of time-domain response) available in the literature.

Controller type	K_P	K_I	K_D	λ	μ
HSFS-FOPID [30]	19.23	6.001	3.0159	0.9934	0.9732
GWO-FOPID [31]	18.328	4.9418	3.2612	0.9998	0.9845
SMA-PID [32]	18.6458	2.5235	3.1921	1	1
AOA-HHO-PID [33]	14.435	0.1636	1.7620	1	1
hASO-SA-PID [34]	18.4258	3.3082	3.1755	1	1

Table 5
Performance evaluation with respect to reported best approaches in terms of time response specifications.

Controller type	Rise time (s)	Settling time (s)	Overshoot (%)	Peak time (s)
GOA-FOPID (novel method)	**0.0188**	**0.0305**	**0**	**0.0440**
HSFS-FOPID [30]	0.0505	0.0766	1.7659	0.1360
GWO-FOPID [31]	0.0488	0.0814	0.3123	0.1530
SMA-PID [32]	0.0491	0.0857	0.0163	0.1750
AOA-HHO-PID [33]	0.0743	0.2508	2.8383	0.1850
hASO-SA-PID [34]	0.0494	0.0866	0.0272	0.1830

6. Conclusion

This paper has ventured into the realm of micro-DC motors, emphasizing the significance of precise speed regulation in their diverse applications. Micro-DC motors, though small in size, wield immense influence across industries like robotics, automotive technology, medical devices, and consumer electronics. The ability to finely control their rotational speed is paramount for efficiency and functionality in these domains. Our exploration delved into the world of micro-DC motors, where control structures such as the PID controller have long held sway. However, the emergence of FOPID controllers has opened new avenues for enhanced control performance, particularly in systems with nonlinear dynamics or time-varying parameters. Motivated by the need for continuous improvement, we introduced the GOA as an innovative tuning instrument for FOPID controllers tailored to micro-DC motor speed regulation. The GOA draws inspiration from the agility of gazelles in nature and has shown remarkable success in various optimization problems. This study harnessed the GOA's power to fine-tune FOPID controller parameters, optimizing them for peak performance. Through rigorous simulations and meticulous statistical analysis, we demonstrated the GOA's efficiency and effectiveness in optimizing FOPID controllers. It consistently achieved superior cost function values and excelled in various time-domain-based performance metrics, reinforcing its potential as a potent tool for micro-DC motor speed regulation. We

examined the dynamic evolution of controller parameters and the cost function, showcasing the GOA's adaptability and its capability to minimize the cost function over iterations. Additionally, we presented the step response of the GOA-tuned FOPID-controlled system, emphasizing its effectiveness in regulating micro-DC motor speed. In a comprehensive comparison with other reported best approaches, our GOA-FOPID method outperformed them in terms of key time response specifications, including rise time, settling time, percent overshoot, and peak time. In conclusion, this study highlights the transformative potential of the GOA in optimizing FOPID controllers for micro-DC motor speed regulation. The adoption of this novel metaheuristic algorithm offers new avenues for advancing the precision and efficiency of micro-DC motor control, ushering in a future of enhanced performance across a spectrum of applications.

Declaration of Competing Interest

The authors declare that they have no known competing financial interests or personal relationships that could have appeared to influence the work reported in this paper.

Data availability

No data was used for the research described in the article.

References

[1] FM Reato, C Ricci, J Misfatto, M Calzaferri, S. Cinquemani, Multi-physics model of DC micro motors for dynamic operations, Sens Actuators A Phys 361 (2023), 114570, https://doi.org/10.1016/j.sna.2023.114570.

[2] Z Wang, Y Zhang, P Yu, N Cao, H. Dintera, Speed Control of Motor Based on Improved Glowworm Swarm Optimization, Computers, Materials & Continua 69 (2021) 503–519, https://doi.org/10.32604/cmc.2021.017624.

[3] E Çelik, N. Öztürk, First application of symbiotic organisms search algorithm to offline optimization of PI parameters for DSP-based DC motor drives, Neural Comput Appl 30 (2018) 1689–1699, https://doi.org/10.1007/s00521-017-3256-5.

[4] W Xie, JS Wang, HB. Wang, PI Controller of Speed Regulation of Brushless DC Motor Based on Particle Swarm Optimization Algorithm with Improved Inertia Weights, editor, in: E Cuevas (Ed.), PI Controller of Speed Regulation of Brushless DC Motor Based on Particle Swarm Optimization Algorithm with Improved Inertia Weights, Math Probl Eng 2019 (2019), 2671792, https://doi.org/10.1155/2019/2671792.

[5] K Premkumar, B V Manikandan, Bat algorithm optimized fuzzy PD based speed controller for brushless direct current motor, Engineering Science and Technology, an International Journal 19 (2016) 818–840, https://doi.org/10.1016/j.jestch.2015.11.004.

[6] Razmjooy N, Vahedi Z, Estrela V V., Padilha R, Monteiro ACB. Speed Control of a DC Motor Using PID Controller Based on Improved Whale Optimization Algorithm. 2021. pp. 153–167. doi:10.1007/978-3-030-56689-0_8.

[7] M He, T Zhang, J Huang, C. Luo, Speed Control Study of Brushless DC motor Based on Fuzzy Optimization PID, IOP Conf Ser Mater Sci Eng 768 (2020), 042013, https://doi.org/10.1088/1757-899X/768/4/042013.

[8] K Premkumar, BV Manikandan, Fuzzy PID supervised online ANFIS based speed controller for brushless dc motor, Neurocomputing 157 (2015) 76–90, https://doi.org/10.1016/j.neucom.2015.01.032.

[9] S Ekinci, D Izci, B. Hekimoğlu, Optimal FOPID Speed Control of DC Motor via Opposition-Based Hybrid Manta Ray Foraging Optimization and Simulated Annealing Algorithm, Arab J Sci Eng 46 (2021) 1395–1409, https://doi.org/10.1007/s13369-020-05050-z.

[10] K Premkumar, B V Manikandan, Speed control of Brushless DC motor using bat algorithm optimized Adaptive Neuro-Fuzzy Inference System, Applied Soft Computing Journal 32 (2015) 403–419, https://doi.org/10.1016/j.asoc.2015.04.014.

[11] W Aribowo, S Supari, B. Suprianto, Optimization of PID parameters for controlling DC motor based on the aquila optimizer algorithm, International Journal of Power Electronics and Drive Systems (IJPEDS) 13 (2022) 216, https://doi.org/10.11591/ijpeds.v13.i1.pp216-222.

[12] D Izci, S. Ekinci, Optimizing Three-Tank Liquid Level Control: Insights from Prairie Dog Optimization, International Journal of Robotics and Control Systems 3 (2023) 599–608, https://doi.org/10.31763/ijrcs.v3i3.1116.

[13] S Ekinci, D Izci, E Eker, L Abualigah, C-L Thanh, S. Khatir, Hunger games pattern search with elite opposite-based solution for solving complex engineering design problems, Evolving Systems (2023), https://doi.org/10.1007/s12530-023-09526-9.

[14] D Izci, S Ekinci, AG. Hussien, Effective PID controller design using a novel hybrid algorithm for high order systems, editor, in: Y Arya (Ed.), Effective PID controller design using a novel hybrid algorithm for high order systems, PLoS One 18 (2023), e0286060, https://doi.org/10.1371/journal.pone.0286060.

[15] V Kumarasamy, V KarumanchettyThottam Ramasamy, G Chandrasekaran, G Chinnaraj, P Sivalingam, NS Kumar, A review of integer order PID and fractional order PID controllers using optimization techniques for speed control of brushless DC motor drive, International Journal of System Assurance Engineering and Management 14 (2023) 1139–1150, https://doi.org/10.1007/s13198-023-01952-x.

[16] A Zamani, SM Barakati, S. Yousofi-Darmian, Design of a fractional order PID controller using GBMO algorithm for load–frequency control with governor saturation consideration, ISA Trans 64 (2016) 56–66, https://doi.org/10.1016/j.isatra.2016.04.021.

[17] A Mughees, SA. Mohsin, Design and Control of Magnetic Levitation System by Optimizing Fractional Order PID Controller Using Ant Colony Optimization Algorithm, IEEE Access 8 (2020) 116704–116723, https://doi.org/10.1109/ACCESS.2020.3004025.

[18] P Warrier, P. Shah, Optimal Fractional PID Controller for Buck Converter Using Cohort Intelligent Algorithm, Applied System Innovation 4 (2021) 50, https://doi.org/10.3390/asi4030050.

[19] AA Jamil, WF Tu, SW Ali, Y Terriche, JM. Guerrero, Fractional-Order PID Controllers for Temperature Control: A Review, Energies 15 (2022) 3800, https://doi.org/10.3390/en15103800.

[20] M D, J K, P Shah, R Sekhar, Fractional order PIλDμ controller for microgrid power system using cohort intelligence optimization, Results in Control and Optimization 11 (2023), 100218, https://doi.org/10.1016/j.rico.2023.100218.

[21] S Ekinci, B Hekimoğlu, D. Izci, Opposition based Henry gas solubility optimization as a novel algorithm for PID control of DC motor, Engineering Science and Technology, an International Journal 24 (2021) 331–342, https://doi.org/10.1016/j.jestch.2020.08.011.

[22] A Rajasekhar, R Kumar Jatoth, A. Abraham, Design of intelligent PID/PIλDμ speed controller for chopper fed DC motor drive using opposition based artificial bee colony algorithm, Eng Appl Artif Intell 29 (2014) 13–32, https://doi.org/10.1016/j.engappai.2013.12.009.

[23] B. Hekimoglu, Optimal Tuning of Fractional Order PID Controller for DC Motor Speed Control via Chaotic Atom Search Optimization Algorithm, IEEE Access 7 (2019) 38100–38114, https://doi.org/10.1109/ACCESS.2019.2905961.

[24] R V Jain, M V Aware, AS. Junghare, Tuning of Fractional Order PID controller using particle swarm optimization technique for DC motor speed control, in: 2016 IEEE 1st International Conference on Power Electronics, Intelligent Control and Energy Systems (ICPEICES), 2016, pp. 1–4, https://doi.org/10.1109/ICPEICES.2016.7853070.

[25] DH Wolpert, WG. Macready, No free lunch theorems for optimization, IEEE Transactions on Evolutionary Computation 1 (1997) 67–82, https://doi.org/10.1109/4235.585893.

[26] JO Agushaka, AE Ezugwu, L. Abualigah, Gazelle optimization algorithm: a novel nature-inspired metaheuristic optimizer, Neural Comput Appl (2022), https://doi.org/10.1007/s00521-022-07854-6.

[27] L Abualigah, A Diabat, RA. Zitar, Orthogonal Learning Rosenbrock's Direct Rotation with the Gazelle Optimization Algorithm for Global Optimization, Mathematics 10 (2022) 4509, https://doi.org/10.3390/math10234509.

[28] S Ekinci, D. Izci, Enhancing IIR system identification: Harnessing the synergy of gazelle optimization and simulated annealing algorithms. e-Prime - Advances in Electrical Engineering, Electronics and Energy 5 (2023), 100225, https://doi.org/10.1016/j.prime.2023.100225.

[29] VK Munagala, RK. Jatoth, Improved fractional PIλDμ controller for AVR system using Chaotic Black Widow algorithm, Computers & Electrical Engineering 97 (2022), 107600, https://doi.org/10.1016/j.compeleceng.2021.107600.

[30] R Saini, G Parmar, R. Gupta, An enhanced hybrid stochastic fractal search FOPID for speed control of DC motor. Fractional Order Systems and Applications in Engineering, Elsevier (2023) 51–67, https://doi.org/10.1016/B978-0-32-390953-2.00011-6.

[31] J Agarwal, G Parmar, R Gupta, A. Sikander, Analysis of grey wolf optimizer based fractional order PID controller in speed control of DC motor, Microsystem Technologies 24 (2018) 4997–5006, https://doi.org/10.1007/s00542-018-3920-4.

[32] D Izci, S. Ekinci, Comparative Performance Analysis of Slime Mould Algorithm For Efficient Design of Proportional–Integral–Derivative Controller, Electrica 21 (2021) 151–159, https://doi.org/10.5152/electrica.2021.20077.

[33] M. Issa, Enhanced Arithmetic Optimization Algorithm for Parameter Estimation of PID Controller, Arab J Sci Eng 48 (2023) 2191–2205, https://doi.org/10.1007/s13369-022-07136-2.

[34] E Eker, M Kayri, S Ekinci, D. Izci, A New Fusion of ASO with SA Algorithm and Its Applications to MLP Training and DC Motor Speed Control, Arab J Sci Eng 46 (2021) 3889–3911, https://doi.org/10.1007/s13369-020-05228-5.

[35] A Harrouz, H Becheri, I Colak, K. Kayisli, Backstepping control of a separately excited DC motor, Electrical Engineering 100 (2018) 1393–1403, https://doi.org/10.1007/s00202-017-0592-5.

[36] Khalilpour M, Razmjooy, N. HH, Moallem P. Optimal Control of DC motor using Invasive Weed Optimization (IWO) Algorithm. Majlesi Conference on Electrical Engineering. Isfahan; 2011. pp. 1–6.

[37] Saini R, Parmar G, Gupta R, Sikander A. An Enhanced Tuning of PID Controller via Hybrid Stochastic Fractal Search Algorithm for Control of DC Motor. 2022. pp. 185–194. doi:10.1007/978-981-16-7274-3_16.

[38] E Çelik, N. Öztürk, A hybrid symbiotic organisms search and simulated annealing technique applied to efficient design of PID controller for automatic voltage regulator, Soft comput 22 (2018) 8011–8024, https://doi.org/10.1007/s00500-018-3432-2.

[39] P Shah, S. Agashe, Review of fractional PID controller, Mechatronics 38 (2016) 29–41, https://doi.org/10.1016/j.mechatronics.2016.06.005.
[40] L Abualigah, S Ekinci, D Izci, R. Abu Zitar, Modified Elite Opposition-Based Artificial Hummingbird Algorithm for Designing FOPID Controlled Cruise Control System, Intelligent Automation & Soft Computing (2023), https://doi.org/10.32604/iasc.2023.040291.
[41] PJ Shaija, AE. Daniel, Optimal Tuning of PI Controllers for IM Drive using GWO and TLBO Algorithms, in: 2023 Fifth International Conference on Electrical, Computer and Communication Technologies (ICECCT), IEEE, 2023, pp. 01–09, https://doi.org/10.1109/ICECCT56650.2023.10179749.
[42] D Izci, S. Ekinci, A novel-enhanced metaheuristic algorithm for FOPID-controlled and Bode's ideal transfer function–based buck converter system, Transactions of the Institute of Measurement and Control 45 (2023) 1854–1872, https://doi.org/10.1177/01423312221140671.



Davut Izci received his BSc degree from Dicle University, Turkey, in Electrical and Electronic Engineering and his MSc and PhD degrees from Newcastle University, England - UK, in Mechatronics and Microsystems, respectively. He is currently an Associate Professor working on optimization, control system design, sensing applications, energy harvesting, microsystems development and applications of metaheuristic optimization techniques to different control systems and real-world engineering problems.



Serdar Ekinci received his BSc degree in Control Engineering, and his MSc and PhD degrees in Electrical Engineering all from Istanbul Technical University (ITU), in 2007, 2010 and 2015, respectively. He is currently an Associate Professor working in Department of Computer Engineering at Batman University, Turkey. His areas of interest are electrical power systems, stability, control technology and the applications of metaheuristic optimization algorithms to various control systems